

oxidation states of tungsten relative to those of molybdenum. Monomeric $\text{LW}^{\text{III}}\text{Cl}_3^-$ complexes, which are obtained by chemical (hydrazine) or electrochemical reduction of $\text{LW}^{\text{IV}}\text{Cl}_3$, react with air in solution but not in the solid state. Structural characterization of the mixed cation salt $(\text{NH}_4)_{0.5}(\text{Et}_4\text{N})_{0.5}\text{HBpz}_3\text{WCl}_3$ (**5**) demonstrates that the anion is monomeric and nearly isostructural with **2**. The ammonium cations are “coordinated” by the six chlorides from two anions in a trigonal antiprismatic geometry with N–Cl distances of 3.24 Å.

With respect to the bioinorganic chemistry of molybdenum this work suggests that (1) the +3 oxidation state should not be ruled out a priori due to incompatibility with biological redox potentials and (2) if Mo(III) is found in biological systems, it very well might be coordinated to histidine residues.¹³

Acknowledgment is made to the donors of the Petroleum Research Fund, administered by the American Chemical Society, for grants to M.M. and S.K.

Supplementary Material Available: Tables of fractional atomic coordinates and thermal parameters (5 pages). Ordering information is given on any current masthead page.

(12) Crystals of compound **5** which display pyritohedral morphology are cubic (*Pa*3, No. 205) with $a = 16.085$ (2) Å and $V = 4161$ Å³. The anion possesses a threefold axis. The ammonium cation lies at special position 4b, while the nitrogen of the NEt_4 cation is at special position 4a. The ethyl groups of this cation are, therefore, substantially disordered. Least-squares refinement using 600 reflections with $I > 3.0\sigma(I)$ of all nonhydrogen atoms excluding the ethyl groups gave $R = 0.061$ and $R_w = 0.094$.

(13) The use of polypyrazolylborate ligands to model the coordination by histidines has been previously recognized: Thompson, J. S.; Marks, T. J.; Ibers, J. A. *J. Am. Chem. Soc.* **1979**, *101*, 4180–4192.

Nuclear Shielding of Trapped Xenon Obtained by Proton-Enhanced, Magic-Angle Spinning ¹²⁹Xe NMR Spectroscopy

John A. Ripmeester

Division of Chemistry
National Research Council of Canada
Ottawa, Ontario, Canada K1A 0R9

Received August 21, 1981

The nuclear shielding of the spin $1/2$ ¹²⁹Xe nucleus (natural abundance 26.24%) is extremely sensitive to its physical environment as shown by its strong dependence on density in the pure phases.^{1,2} Using such solid-state NMR techniques as ¹H dipolar decoupling,³ ¹²⁹Xe–¹H cross-polarization,³ and magic-angle spinning,^{4,5} several examples of the ¹²⁹Xe NMR “physical shift” are illustrated. For trapped xenon atoms it is shown that the nuclear shielding and shielding anisotropy depend on the nature of the trapping site.

Figure 1a–c shows the ¹²⁹Xe NMR spectrum⁶ of xenon atoms trapped in the cages of the β -quinol clathrate.⁷ The line shape shown in Figure 1a, obtained by using single pulses and without

- (1) D. Brinkman and H. Y. Carr, *Phys. Rev.*, **150**, 174 (1966).
- (2) C. J. Jameson, A. K. Jameson, and S. M. Cohen, *J. Chem. Phys.*, **62**, 4224 (1975).
- (3) A. Pines, M. C. Gibby, and J. S. Waugh, *J. Chem. Phys.*, **59**, 569 (1973).
- (4) J. Schaefer, S. H. Chin, and S. I. Weissman, *Macromolecules*, **5**, 798 (1972).
- (5) J. Schaefer, E. O. Stejskal, and R. Buchdahl, *Macromolecules*, **10**, 384 (1977).
- (6) ¹²⁹Xe NMR spectra were obtained at 49.8 MHz using a Bruker CXP-180 NMR spectrometer. 500 or 1k datum points (sweep width 50 kHz) were collected after a single pulse or a single matched cross-polarization sequence before zero filling and Fourier transformation. Radio-frequency field amplitudes were ~ 30 kHz. For the magic-angle spinning experiments, a Kel-F rotor of the Andrew type was used at spinning frequencies of 2.5–3 kHz.
- (7) H. M. Powell in “Non-Stoichiometric Compounds”, L. Mandelcorn, Ed., Academic Press, New York, 1964. The β -quinol sample used had $\sim 60\%$ of the cages occupied with Xe.

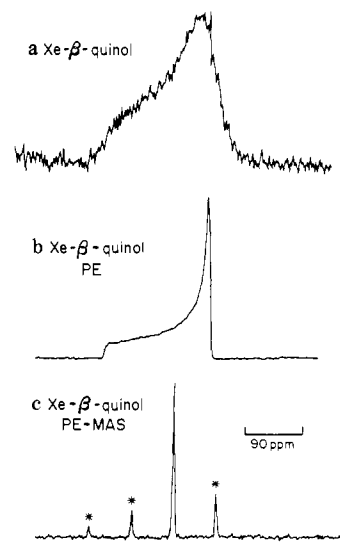


Figure 1. ¹²⁹Xe NMR spectrum of xenon trapped in β -quinol. (a) Obtained using 120 (N_s) single pulses at 12-min repetition rate (τ_r); (b) obtained using proton enhancement (PE) cross-polarization time (τ_{cp}) of 30 ms, $\tau_r = 60$ s, $N_s = 80$; (c) obtained using proton enhancement (PE) and magic angle spinning (MAS), $N_s = 24$, $\tau_{cp} = 30$ ms, $\tau_r = 60$ s.

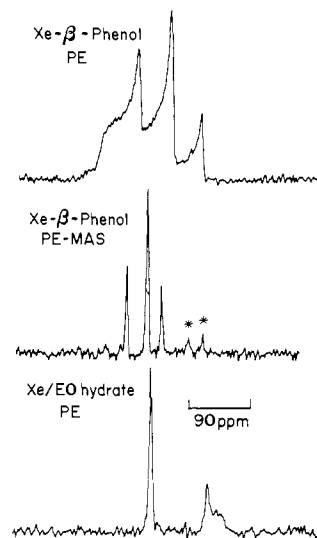


Figure 2. (a), (b) PE and PE-MAS ¹²⁹Xe NMR spectrum of xenon in β -phenol, $\tau_{cp} = 10$ ms, $\tau_r = 30$ s for (a), $N_s = 106$, for (b) $N_s = 40$; (c) PE ¹²⁹Xe NMR spectrum of xenon in a mixed structure I hydrate of ethylene oxide and xenon, $N_s = 40$, $\tau_{cp} = 0.8$ ms, $\tau_r = 30$ s.

Table I. Summary of ¹²⁹Xe Nuclear Shielding

sample	σ , ppm ^a	$\Delta\sigma$, ppm
β -quinol	–222	–160
β -phenol small cage	–229	–171
large cage site I	–250	–105
large cage site II	–279	–53
Xe/EO structure I hydrate		
small cage	–240	
large cage	–150	30

^a Referred to Xe gas at zero density.

¹H decoupling, required an accumulation time of 24 h, whereas the line shape in Figure 1b, obtained by using ¹²⁹Xe–¹H cross-polarization and ¹H dipolar decoupling, required only 1.5 h⁸ and thus nicely illustrates some of the advantages of the second techniques. The cages in the β -quinol clathrate of ~ 4.2 -Å free diameter have $\bar{3}$ symmetry and are elongated slightly along the

(8) The protons are probably relaxed quite efficiently by spin diffusion to paramagnetic centers. The ¹²⁹Xe atoms, being quite dilute, do not have such a mechanism so that extremely long T_1 s result.

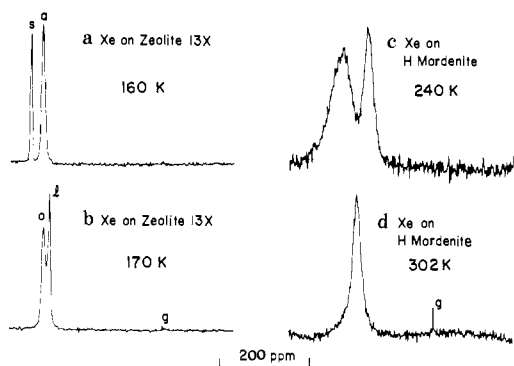


Figure 3. (a), (b) ^{129}Xe NMR spectrum of excess xenon on Linde 13X zeolite, obtained using 40 single pulses at 40-s repetition rate; lines due to solid, liquid, gaseous, and adsorbed xenon are labeled s, l, g, and a respectively; (c), (d) ^{129}Xe NMR spectrum of xenon in hydrogen mordenite obtained using 400 single pulses at 4-s repetition rate.

symmetry axis.⁷ The ends of the cages are formed by hexagonal rings consisting of six hydrogen-bonded OH units, the phenyl groups forming the cage walls. The ^{129}Xe line shape is characteristic of an axial shielding tensor with $\Delta\sigma = 160$ ppm so that the shielding along the cage axis is greater than that perpendicular to the axis. Figure 1c shows that on spinning the Xe- β -quinol sample at the magic angle at ~ 2.5 kHz, the powder pattern is reduced to a single line at the average shielding value, 222 ppm with respect to xenon gas at zero density, plus several spinning side bands.

Figure 2a, the ^{129}Xe spectrum obtained for xenon trapped in the phenol clathrate,⁹ consists of three overlapping axially symmetric powder patterns. The spectrum obtained when the sample is spun at the magic angle is shown in Figure 2b; the average shielding and shielding anisotropies are summarized in Table I. There are two kinds of cages in the phenol clathrates, one similar in shape and size to the β -quinol cage and the other an elongated, axially symmetric cage of length ~ 15 Å and diameter 4.3 Å which can hold three xenon atoms, one next to each hexagonal (OH)₆ ring at the ends of the cage and one in between these two. The three lines can then be assigned as follows: The high field line, with shielding parameters similar to the β -quinol line, can be assigned to xenon in the small cages; the most intense middle line to the xenons in the large cage near the hexagonal rings, and the low field line to the central xenon in the large cage.

Figure 2c shows the ^{129}Xe NMR spectrum obtained for a structure I clathrate hydrate¹⁰ containing ethylene oxide (EO) and xenon as guest molecules. The larger EO molecules occupy mainly the large cages; the xenon is distributed between the large and small cages. The low field line corresponds to xenon atoms in the small, nearly spherical structure I cages of $m\bar{3}$ symmetry and 3.91-Å free diameter. The high field line can be assigned to xenon in the large cage, an oblate spheroid of $\bar{4}2m$ symmetry and ~ 4.33 -Å free diameter. In this case the shielding along the cage axis is less than the shielding perpendicular to the axis.

Figure 3a,b shows the Xe spectra of a dehydrated sample¹¹ of zeolite 13X containing excess xenon. Separate signals can be seen for liquid, solid, gaseous, and sorbed xenon. At 160 K the bulk xenon not trapped in the zeolite is frozen, and its NMR signal is shifted to low field of the sorbed xenon line. Since the total amount of xenon in the sample is known and the two lines are completely resolved (Figure 3a), the integrated line intensities can be used to calculate the zeolite cage occupancy. In this instance, there were found to be 10-11 xenon atoms per cage, assuming that all xenon atoms occupy only the zeolite supercages. Evidently sorbed xenon does not freeze at the bulk xenon melting point.

(9) M. Von Stackelberg, A. Hoverath, and C. Scheringer, *Z. Elektrochem.*, **62**, 123 (1958).

(10) D. W. Davidson in "Water, a Comprehensive Treatise", F. Franks, Ed., Plenum Press, New York, 1975.

(11) A commercial sample of Linde 13 X zeolite was dehydrated at 400 °C under vacuum.

Above the melting point, the liquid line shifts to high field of the sorbed xenon line. This suggests that the sorbed xenon may be considered to be a liquid somewhat denser than bulk liquid xenon.

Figures 3c and 3d show spectra for xenon sorbed on a hydrogen mordenite sample.¹² At 240 K, two relatively broad lines are evident, ~ 62 ppm apart. The low field line can be assigned to xenon in the side pockets of the mordenite and the high field line to xenon in the main channel. Evidently at 240 K there is no exchange of the two types of xenon. The relatively large line widths suggest that within the two types of sites there is a further distribution. At 302 K only a single line is observable so that the xenon in the main channel and the side pockets are in a state of rapid exchange.

The Xe resonances reported here and for the condensed phases all occur to the low field of the infinitely dilute gas line. The shielding of the atom with respect to the bare nucleus has been estimated to be $\sigma = 5642$ ppm,¹³ the degree of shielding being reduced by the effect of collisions and electron overlap with adjacent molecules.

The intensity information derived from Xe NMR spectra allows the measurement of the occupancy of inequivalent sites and should allow the testing and refining of guest-host potential functions. A detailed discussion of the potential functions for clathrate hydrates will be given elsewhere.¹⁴ The measurements presented for the porous solids suggest that Xe NMR spectroscopy may be used to good advantage to study both the nature of porous crystals and the dynamics of Xe sorbed in such systems. Extensions to the study of phase transitions in surface layers and thin films are also indicated.

(12) An ammonium mordenite was prepared by ion exchange from commercial sodium mordenite (Strem Chemical Co.) This was then calcined at 500 °C in air to yield the hydrogen form.

(13) G. Malli and C. Froese, *Int. J. Quantum Chem.*, **1**, 95 (1967).

(14) J. A. Ripmeester and D. W. Davidson, *J. Mol. Struct.*, **75**, 67 (1981). J. S. Tse and D. W. Davidson, *ACS Symp. Series*, in press.

Organophosphorus Compounds: The First Applications of Sulfuryl Chloride Fluoride SO_2FCl in Synthesis

Andrzej Łopusiński and Jan Michalski*

Polish Academy of Sciences
Centre of Molecular and Macromolecule Studies
90-362 Lodz, Boczna 5, Poland

Received July 6, 1981

Although sulfuryl chloride fluoride SO_2FCl (1) is readily available¹ and has been used as a solvent,² its chemistry is almost unexplored. Our previous work on the reaction between sulfuryl chloride and esters 2 (X = S)³ suggested that 1 should be useful for converting compounds 2 and related systems into fluoridates $\text{RR}'\text{P}(\text{O})\text{F}$ (3) and fluorophosphoranes R_3PF_2 (5). We now report that the reaction between compounds $\text{>P}=\text{X}$ and sulfuryl chloride fluoride makes available a variety of fluorinated organophosphorus compounds, including new potential enzyme inhibitors.

The thione derivatives 2 (R, R' = alkyl or alkoxy, X = S) with sulfuryl chloride fluoride in methylene chloride for 30 min at -78

(1) Tullock, C. W.; Coffman, D. D. *J. Org. Chem.* **1960**, *25*, 2016.

(2) Olah, G. A.; Bruce, M. R. *J. Am. Chem. Soc.* **1979**, *101*, 4765. Olah, G. A.; Bruce, M. R.; Clouet, F. L. *J. Org. Chem.* **1981**, *46*, 438.

(3) Skowrońska, A.; Mikolajczak, J.; Michalski, J. *J. Am. Chem. Soc.* **1978**, *100*, 5386.

(4) ^{31}P NMR spectroscopy with an external H_3PO_4 reference. Negative chemical shift values indicate absorption at higher fields than H_3PO_4 . ^{19}F NMR spectroscopy with internal CFCl_3 reference.

(5) The cis-trans geometry for 2-fluoro-2-oxo-4-methyl-1,3,2-dioxaphosphorinans (7) and the axial preference of fluorine at phosphorus was established by: Okruszek, A.; Stec, W. J. *Z. Naturforsch. B* **1976**, *31b*, 354.

(6) Schmutzler, R. *Angew. Chem.* **1965**, *77*, 530.